Metrol. Meas. Syst., Vol. 32 (2025) No. 2, pp. 1–20
DOI: 10.24425/mms.2023.154342

METROLOGY AND MEASUREMENT SYSTEMS
Index 330930, ISSN 0860-8229
www.metrology.wat.edu.pl

AN ALGORITHM FOR FAST UNCERTAINTY EVALUATION IN RMS VOLTAGE MEASUREMENT

Sergiusz Sienkowski[1], Mariusz Krajewski[1], Jadwiga Lal-Jadziak[2]

1) Institute of Metrology, Electronics and Computer Science, University of Zielona Góra, Szafrana 2, 65–516 Zielona Góra, Poland (✉ *s.sienkowski@imei.uz.zgora.pl*)
2) Institute of Engineering and Technology, Nicolaus Copernicus University of Toruń, 87-100 Toruń, Poland

Abstract

This paper presents a new algorithm for fast uncertainty evaluation of root mean square (RMS) voltage measurement. It enables the evaluation of the expanded measurement uncertainty and partial uncertainties, which are useful in metrological analysis of the measurement. It can be used for any measurement system in which the RMS value is determined based on voltage samples. Various sources of uncertainty have been considered for this measurement system. The proposed algorithm is easier to implement than the commonly used uncertainty propagation method. Its operating principle is based on the Monte Carlo method. However, it allows the computation of the RMS measurement uncertainty within a significantly shorter time compared to the classical Monte Carlo method. The simulation and experimental results presented in this paper confirm the correct operation of the new algorithm and the acceleration of uncertainty computations up to 200 times in RMS measurement based on 1000 voltage samples.

Keywords: Algorithm, measurement uncertainty evaluation, Monte Carlo method, RMS voltage, uncertainty budget.

1. Introduction

The effective value of electric voltage, usually called the *root mean square* (RMS) voltage, is one of the basic quantities measured in electrical engineering and automation [1]. Both RMS measurement methods and their uncertainties have been the subject of numerous publications [2–13]. RMS measurement methods based on voltage samples are gaining popularity in the technology [6–10].

In a scenario where the measured effective value is determined based on samples of the analysed voltage, estimating the measurement uncertainty is not straightforward. In such cases, the measurement results are influenced by various sources of uncertainty [6–9]. In addition, each sample should be treated as a separate measurement of the instantaneous voltage. Therefore, determining the measurement uncertainty using the classical method according to the Guide [14], *i.e.* applying the law of uncertainty propagation, is inherently difficult and complex. For such intricate measurements, the *Monte Carlo* (MC) method [15], which is simpler to implement,

Article history: received September 19, 2024; revised November 12, 2024; accepted December 10, 2024; available online April 22, 2025.

can be applied, as in [6] or [16]. The drawback of this method (hereinafter, referred to as the classical MC method) in evaluating the uncertainty of the effective value is the large number of iterations required, which results in a relatively long computational time. The computational time is important in scientific and design studies, where a large amount of data is aggregated and processed in assessing the uncertainty. Therefore, it is essential to accelerate the computations and obtain reliable and repeatable uncertainty results.

The problem of the relatively long computational time of RMS measurement uncertainty has not been addressed in the literature, which inspired the authors of this paper to tackle this issue. For this reason, the authors have developed a new algorithm to significantly accelerate the evaluation of uncertainty.

The new algorithm is also based on the MC method. However, it significantly reduces the computational time compared to the classical MC method. This algorithm enables the evaluation of the measurement uncertainty of the effective value determined based on the root mean square value of samples collected at a time corresponding to a multiple of the period of the analysed alternating voltage. The advantage of the proposed algorithm and classical MC method over the uncertainty propagation method [14] is the ability to analyse uncertainties in the form of intervals that do not need to be symmetric with respect to zero.

To verify and compare the operation of the proposed algorithm with that of the classical MC method [6, 15], the authors conducted studies to evaluate the expanded uncertainty intervals for various measurement scenarios. In addition, the authors created an uncertainty budget for a measurement system example. The uncertainty budget makes it possible to analyse the effect of the sources of uncertainty on the measurement results and indicate which effects should be reduced to achieve better results. This approach is crucial for precise measurements, where the aim is to eliminate the sources of uncertainty [6–8]. In this research, the authors assumed that the sources of uncertainty were the parameters errors and digital processing errors of sinusoidal voltage. These errors included the fundamental voltage measurement error, frequency error, and sampling frequency error. The uncertainty was also influenced by the initial phase of the voltage, zero error (offset), and accompanying noise.

The paper consists of six sections and two appendices (A and B). Section 2 defines the concept of the effective value of the sinusoidal electric voltage and presents the obtained analytical equations. Section 3 introduces a new algorithm for fast evaluation of the expanded measurement uncertainty of the effective value. Section 4 presents the simulation and experimental results. In Section 5, the authors evaluate the computational time of the proposed algorithm. The authors summarise the study in Section 6. The appendices and the cited references are provided at the end of this paper.

2. Effective value

Similarly to the works [6–9], it was assumed that the effective value of the sinusoidal voltage is measured with a constant or random initial phase and the voltage is accompanied by disturbances in the form of a DC component and Gaussian noise. On this basis, let us consider a measurement system enabling the acquisition of a sinusoidal electric voltage:

$$v_0(t) = V_m \sin\left(2\pi f t + \varphi\right), \quad 0 \le t \le T, 0 < T < \infty, \tag{1}$$

where V_m, φ, f and T are respectively the amplitude, initial phase, frequency, and period of the voltage.

*Metrol. Meas. Syst.,*Vol. 32 (2025), No. 2, pp. 1–20
DOI: 10.24425/mms.2023.154342

Let us assume that the voltage $v_0(t)$ is accompanied by a DC component V_0 and an independent additive Gaussian noise $q(t)$ with a fixed expected value μ_q and standard deviation σ_q. In this way, we obtain the voltage:

$$v(t) = v_0(t) + q(t) + V_0 = V_m \sin(2\pi f t + \varphi) + q(t) + V_0. \tag{2}$$

If $v(t)$ is uniformly sampled with a sampling frequency f_s, then the samples $v[n]$ of the voltage can be described by the formulas:

$$v[n] = v_0[n] + q[n] + V_0, \quad n = 0, 1, \ldots, M-1, \tag{3}$$

$$v_0[n] = V_m \sin(\omega_0 n + \varphi), \tag{4}$$

where:

$$\omega_0 = 2\pi \frac{f}{f_s}, \quad 0 < \omega_0 \le \pi, \tag{5}$$

wherein $v_0[n]$ and $q[n]$ are samples of the signal $v_0(t)$ and noise $q(t)$, respectively.

Let us denote by $\mathrm{RMS_e}$ the estimator of the effective value (RMS value). To compute $\mathrm{RMS_e}$ the generalised mean can be employed:

$$\hat{\mathrm{m}}(\mathbf{s}, r) = \left(\frac{1}{M}\sum_{n=0}^{M-1}(s[n])^r\right)^{\frac{1}{r}}, \tag{6}$$

where r is an affinely extended real number [17], and $\mathbf{s}$ is an M-element vector of samples $s[n]$ of a periodically varying voltage $s(t)$. Let us assume that:

$$\mathrm{RMS_e} = \hat{\mathrm{m}}(\mathbf{v}, 2) \tag{7}$$

is an estimator of the parameter:

$$\mathrm{RMS} = \sqrt{P_{v_0}}, \tag{8}$$

calculated from (6) and M-element vector $\mathbf{v}$ of samples $v[n]$ of the voltage $v(t)$, where:

$$P_{v_0} = \frac{V_m^2}{2} \tag{9}$$

is the mean power of the voltage $v_0(t)$. Then the $\mathrm{RMS_e}$ estimator is biased and has non-zero variance (see Appendix A), *i.e.*:

$$\begin{aligned} \mathrm{b}[\mathrm{RMS_e}] \approx{}& \sqrt{(\mu_q + V_0)^2 + (\hat{\mathrm{m}}(\mathbf{v_0}, 2))^2 + 2(\mu_q + V_0)\,\hat{\mathrm{m}}(\mathbf{v_0}, 1)} - \mathrm{RMS} \\ &+ \frac{\sigma_q^2}{2\sqrt{(\mu_q + V_0)^2 + (\hat{\mathrm{m}}(\mathbf{v_0}, 2))^2 + 2(\mu_q + V_0)\,\hat{\mathrm{m}}(\mathbf{v_0}, 1)}}\left(1 - \frac{1}{M}\right), \end{aligned} \tag{10}$$

$$\mathrm{Var}[\mathrm{RMS_e}] \approx \frac{\sigma_q^2}{M}, \tag{11}$$

where $\mathbf{v_0}$ is an M-element vector of samples $v_0[n]$ from formula (4).

Let:

$$\mathrm{P} = \mathrm{RMS_e^2} \tag{12}$$

be an estimator of the mean power P_{v0} from formula (9). If we substitute (3) into (12), the power P can be brought to the following form:

$$\begin{aligned}\mathrm{P} &= V_0^2 + \frac{1}{M}\sum_{n=0}^{M-1}(v_0[n])^2 + \frac{2V_0}{M}\sum_{n=0}^{M-1}v_0[n] + \frac{2V_0}{M}\sum_{n=0}^{M-1}q[n] \\ &+ \frac{1}{M}\sum_{n=0}^{M-1}(q[n])^2 + \frac{2}{M}\sum_{n=0}^{M-1}v_0[n]q[n] \\ &= \mathrm{P}_v + 2V_0\mathrm{m}_q + \mathrm{P}_q + \frac{2}{M}\mathbf{v_0}^T\mathbf{q},\end{aligned} \tag{13}$$

where $\mathbf{q}$ is an M-element vector of samples $q[n]$, and $\mathbf{v_0}^T\mathbf{q}$ is the scalar product of vectors $\mathbf{v_0}$ and $\mathbf{q}$. Moreover:

$$\mathrm{P}_v = V_0^2 + \rho_P + 2V_0\rho_m, \tag{14}$$

$$\mathrm{m}_q = \hat{\mathrm{m}}(\mathbf{q}, 1), \tag{15}$$

$$\mathrm{P}_q = (\hat{\mathrm{m}}(\mathbf{q}, 2))^2, \tag{16}$$

where:

$$\rho_m = \frac{V_m}{M}\frac{\sin\left(\frac{M}{2}\omega_0\right)}{\sin\left(\frac{\omega_0}{2}\right)}\sin\left(\frac{M-1}{2}\omega_0 + \varphi\right), \tag{17}$$

$$\rho_P = \begin{cases}\frac{V_m^2}{2} - \frac{V_m^2}{2M}\frac{\sin(M\omega_0)}{\sin(\omega_0)}\cos((M-1)\omega_0 + 2\varphi), & \sin(\omega_0) \neq 0, \\ V_m^2\sin^2(\varphi), & \text{otherwise}.\end{cases} \tag{18}$$

Let $\mathbf{q_0}$ be the vector of samples $q_0[n] = q[n] - \mu_q$. Then the formula (13) takes the form:

$$\begin{aligned}\mathrm{P} &= (V_0 + \mu_q)^2 + \frac{1}{M}\sum_{n=0}^{M-1}(v_0[n])^2 + \frac{2V_0}{M}\sum_{n=0}^{M-1}v_0[n] + \frac{2\mu_q}{M}\sum_{n=0}^{M-1}v_0[n] \\ &+ \frac{2V_0}{M}\sum_{n=0}^{M-1}q_0[n] + \frac{1}{M}\sum_{n=0}^{M-1}(q_0[n])^2 + \frac{2\mu_q}{M}\sum_{n=0}^{M-1}q_0[n] + \frac{2}{M}\sum_{n=0}^{M-1}v_0[n]q_0[n].\end{aligned} \tag{19}$$

Analogously to (13), the formula (19) can be transformed into the following form:

$$\mathrm{P} = (V_0 + \mu_q)^2 + \rho_P + 2V_0\rho_m + 2\mu_q\rho_m + 2V_0\mathrm{m}_{q_0} + \mathrm{P}_{q_0} + 2\mu_q\mathrm{m}_{q_0} + \frac{2}{M}\mathbf{v_0}^T\mathbf{q_0}, \tag{20}$$

where:

$$\mathrm{m}_{q_0} = \hat{\mathrm{m}}(\mathbf{q_0}, 1), \tag{21}$$

$$\mathrm{P}_{q_0} = (\hat{\mathrm{m}}(\mathbf{q_0}, 2))^2. \tag{22}$$

After rearranging formula (20), we obtain:

$$\mathrm{P} = (V_0 + \mu_q)^2 + \rho_P + 2(V_0 + \mu_q)\rho_m + c, \tag{23}$$

where:

$$c = \mathrm{P}_{q_0} + 2\left(V_0 + \mu_q\right)\mathrm{m}_{q_0} + \frac{2}{M}\mathbf{v_0}^T\mathbf{q_0}. \tag{24}$$

If M is sufficiently large, then:

$$\mathrm{P} \approx \left(\mu_q + V_0\right)^2 + \rho_P + 2\left(\mu_q + V_0\right)\rho_m + \sigma_q^2. \tag{25}$$

We observe that if the sampling is coherent (the samples are collected within a measurement window corresponding to an integer number of voltage periods), then $\rho_m = 0$ and $\rho_P = P_{v0}$. In this case, $\mathrm{P} \approx (\mu_q + V_0)^2 + P_{v0} + \sigma_q^2$. However, if $v(t)$ is sampled at the Nyquist frequency, $i.e. f_s = 2f$ and $\varphi = l\pi$, $l = 0, 1, 2$, then $\rho_m = \rho_P = 0$ and $\mathrm{P} \approx (\mu_q + V_0)^2 + \sigma_q^2$.

The performed operations resulted in the extraction of components c and σ_q^2 from (23) and (25) associated with $q(t)$ in the estimator P. This allowed for the development of a new algorithm for fast evaluation of the expanded uncertainty in a system for measurement of the effective value.

3. Algorithm for fast evaluation of the measurement uncertainty of the effective value

The proposed algorithm and classical MC method operate on the data obtained using the procedure shown in Table 1. The input parameters (**Input data**) of the procedure include sinusoidal voltage parameters, digital processing parameters, limiting errors δV_m^*, δf^*, δf_s^* (expressed in %), ΔV_0^* (expressed in V) of these parameters, and the number of experimental repetitions K. These errors are determined based on the documentation of a measuring equipment. In practice, it is often assumed that the expected value of the Gaussian noise is equal to zero. Therefore, we assume that $\mu_q = 0$ when the data are generated.

Table 1. Data generation procedure.

Input data: V_m, SNR, δV_m^*, δf^*, δf_s^*, ΔV_0^*, K.	
Step 1.	Calculate: (a) mean power P_{v0} based on (9) and V_m; (b) RMS value based on (8) and P_{v0}; (c) standard deviation σ_q based on (26), P_{v0} and SNR.
Step 2.	Generate K – element vectors $\mathbf{\delta V_m}$, $\mathbf{\delta f}$, $\mathbf{\delta f_s}$, $\mathbf{V_0}$ and $\boldsymbol{\varphi}$ based on (27), δV_m^*, δf^*, δf_s^* and ΔV_0^*.
Output data: $\mathbf{\delta V_m}$, $\mathbf{\delta f}$, $\mathbf{\delta f_s}$, $\mathbf{V_0}$, $\boldsymbol{\varphi}$, σ_q, RMS.	

In Step 1, the power P_{v0}, RMS value and standard deviation of the Gaussian noise are calculated as follows:

$$\sigma_q = \sqrt{\mathrm{P}_{v_0} \cdot 10^{-\frac{\mathrm{SNR}}{10}}}, \tag{26}$$

where SNR is the signal-to-noise ratio expressed in decibels (dB). In Step 2, vectors $\mathbf{\delta V_m}$, $\mathbf{\delta f}$, $\mathbf{\delta f_s}$, $\mathbf{V_0}$, and $\boldsymbol{\varphi}$ are generated, consisting of K elements $\delta\hat{V}_m$, $\delta\hat{f}$, $\delta\hat{f}_s$, $\hat{V}_0$ and $\boldsymbol{\varphi}$, with:

$$\begin{aligned}&\delta\hat{V}_m \sim \mathbf{R}\left[-\delta V_m^*, \delta V_m^*\right], \quad \delta\hat{f} \sim \mathbf{R}\left[-\delta f^*, \delta f^*\right], \quad \delta\hat{f}_s \sim \mathbf{R}\left[-\delta f_s^*, \delta f_s^*\right],\\ &\hat{V}_0 \sim \mathbf{R}\left[-\Delta V_0^*, \Delta V_0^*\right], \quad \varphi \sim \mathbf{R}[0, 2\pi].\end{aligned} \tag{27}$$

From formula (27), it follows that the elements of the vectors are random numbers with a rectangular (uniform) distribution $\mathbf{R}[a, b]$, where a and b are the endpoints of the interval. The obtained data are used as the output of the procedure (**Output data**).

Table 2 presents our new algorithm for fast evaluation of the measurement uncertainty of the effective value. The algorithm is based on formulas (23) and (25). Because formula (23) involves an iterative component c and formula (25) underestimates P_{v0}, to accelerate the computations and avoid underestimation, we propose to replace c with the correction $\hat{c}$, which is a random number with a normal (Gaussian) distribution:

$$\hat{c} \sim \mathbf{N}\left(\mu_P, \sigma_P\right), \tag{28}$$

where the mean value μ_P and the standard deviation σ_P are equal, as follows:

$$\mu_P = \sigma_q^2, \quad \sigma_P = \frac{2}{\sqrt{M}}\sigma_q\sqrt{\mu_q^2 + \hat{\mathrm{P}}_v + 2\mu_q\hat{\mathrm{m}}_v + \frac{1}{2}\sigma_q^2}. \tag{29}$$

Table 2. Algorithm for fast evaluation of measurement uncertainty of the effective value.

Input data: $\boldsymbol{\delta}\mathbf{V_m}$, $\boldsymbol{\delta}\mathbf{f}$, $\boldsymbol{\delta}\mathbf{f_s}$, $\mathbf{V_0}$, $\boldsymbol{\varphi}$, V_m, f, f_s, RMS, K, p, M, σ_q;	
Step 1.	Assume $k = 1$.
Step 2.	Determine: (a) parameters $\hat{V}_m$ and $\hat{\omega}_0$ based on (30), V_m, f, f_s, and k-th elements $\delta\hat{V}_m$, $\delta\hat{f}$, $\delta\hat{f}_s$ of vectors $\boldsymbol{\delta}\mathbf{V_m}$, $\boldsymbol{\delta}\mathbf{f}$, $\boldsymbol{\delta}\mathbf{f_s}$; ($b$) coefficients $\hat{\rho}_m$ and $\hat{\rho}_P$ based on (17), (18), $\hat{V}_m$, $\hat{\omega}_0$, M, and k-th element φ of vector $\boldsymbol{\varphi}$; (c) power $\hat{\mathrm{P}}_v$ based on (14), $\hat{\rho}_m$, $\hat{\rho}_P$ and k-th element $\hat{V}_0$ of vector $\mathbf{V_0}$.
Step 3.	Generate correction $\hat{c}$ based on (28), (33), $\hat{\mathrm{P}}_v$, σ_q, and M.
Step 4.	Calculate: (a) power P based on (32), $\hat{\rho}_m$, $\hat{\rho}_P$, $\hat{c}$ and k-th element $\hat{V}_0$ of vector $\mathbf{V_0}$; (b) estimator $\mathrm{RMS_e}$ based on (34) and P.
Step 5.	Determine the error Δ_{RMS} based on (35), $\mathrm{RMS_e}$, and RMS. Store Δ_{RMS}.
Step 6.	Assume $k = k + 1$. If $k \leq K$, repeat steps 2 – 5. If $k > K$, create K-element vector $\boldsymbol{\Delta}_{\mathbf{RMS}}$ based on stored Δ_{RMS}.
Step 7.	Evaluate the endpoints U_{low} and U_{high} of the expanded uncertainty interval based on [15] and $\boldsymbol{\Delta}_{\mathbf{RMS}}$, K, p. Calculate the mean value $\mathrm{m}_{\Delta\mathrm{RMS}}$ and standard deviation $\sigma_{\Delta\mathrm{RMS}}$ from $\boldsymbol{\Delta}_{\mathbf{RMS}}$.
Output data: U_{low}, U_{high}, $\mathrm{m}_{\Delta\mathrm{RMS}}$, $\sigma_{\Delta\mathrm{RMS}}$.	

The components $\hat{\mathrm{P}}_v$ and $\hat{\mathrm{m}}_v$ in formula (29) are calculated based on formulas (14) and (A.14) For this purpose, we use coefficients $\hat{\rho}_m$ and $\hat{\rho}_P$ determined based on formulas (17) and (18) as well as parameters M, φ, and $\hat{V}_0$, as follows:

$$\hat{V}_m = V_m\left(1 + \frac{\delta\hat{V}_m}{100}\right), \quad \hat{\omega}_0 = 2\pi\frac{f\left(1 + \dfrac{\delta\hat{f}}{100}\right)}{f_s\left(1 + \dfrac{\delta\hat{f}}{100}\right)}, \tag{30}$$

where $\delta\hat{V}_m$, $\delta\hat{f}$, $\delta\hat{f}_s$, $\hat{V}_0$, and φ are given by formula (27).

In this manner, we obtain a non-iterative estimator:

$$\mathrm{P} \approx \left(\hat{V}_0 + \mu_q\right)^2 + \hat{\rho}_P + 2\left(\hat{V}_0 + \mu_q\right)\hat{\rho}_m + \hat{c} \tag{31}$$

of power P_{v0}. Since we assume $\mu_q = 0$,

$$\mathrm{P} \approx \hat{V}_0^2 + \hat{\rho}_P + 2\hat{V}_0\hat{\rho}_m + \hat{c} = \hat{\mathrm{P}}_v + \hat{c}, \tag{32}$$

where $\hat{\mathrm{P}}_v$ is derived from formula (14). In addition, the correction parameters in (28) take the following forms:

$$\mu_P = \sigma_q^2, \quad \sigma_P = \sqrt{\frac{2}{M}}\sigma_q\sqrt{2\hat{\mathrm{P}}_v + \sigma_q^2}. \tag{33}$$

DOI: 10.24425/mms.2023.154342

The correction in formula (28) was developed by calculating the variance Var [P] of the estimator P from formula (12) (see Appendix B). This correction eliminates the possibility of underestimating P due to failure to include the components, caused by the noise $q(t)$ appearing in the voltage $v(t)$, in formula (25). Based on the variance, the standard deviation σ_P is determined from formula (29). The form of parameter μ_P, however, results from formula (25). In this manner, data can be generated whose parameters (*i.e.* variance and expected value) correspond to the parameters of the data obtained by calculating c from formula (24).

The proposed algorithm is executed in seven steps. The input data for the algorithm are obtained based on the procedure shown in Table 1 (**Output data**). As the algorithm is based on the MC method, it considers the coverage probability $p \in (0, 1)$ and K, assuming that $K > 10^4/(1-p)$ [15].

After initialising the algorithm (Step 1), the parameters $\hat{V}_m$, $\hat{\omega}_0$, $\hat{\rho}_m$, $\hat{\rho}_P$, and $\hat{\mathrm{P}}_v$ are determined (Step 2). In Step 3, the value of correction (28) is generated. After determining the correction (Step 4), the power P is calculated based on formula (32) and the $\mathrm{RMS_e}$ is calculated based on the following formula:

$$\mathrm{RMS_e} = \sqrt{\mathrm{P}}. \tag{34}$$

Then, the error:

$$\Delta_{\mathrm{RMS}} = \mathrm{RMS_e} - \mathrm{RMS} \tag{35}$$

of the estimator $\mathrm{RMS_e}$ of the RMS parameter is determined and stored (Step 5). The process of determining the error in formula (35) is repeated $K-1$ times (Step 6). As a result of this operation, a vector of errors $\boldsymbol{\Delta}_{\mathbf{RMS}}$ is obtained. In the last step (Step 7), the endpoints U_{low} and U_{high} of the coverage interval of the effective value measurement error are evaluated based on the recommendations of [15] using $\boldsymbol{\Delta}_{\mathbf{RMS}}$, K, and p. Furthermore, based on $\boldsymbol{\Delta}_{\mathbf{RMS}}$, the mean value $\mathrm{m}_{\Delta\mathrm{RMS}}$ and the standard deviation $\sigma_{\Delta\mathrm{RMS}}$ are calculated. The results of the algorithm are U_{low}, U_{high}, $\mathrm{m}_{\Delta\mathrm{RMS}}$, and $\sigma_{\Delta\mathrm{RMS}}$ (**Output data**). Because RMS is known from formula (8), then coverage interval $(U_{\mathrm{low}}, U_{\mathrm{high}})$ can be treated as the expanded uncertainty interval of the effective value measurement based on the estimator (34) for coverage probability p.

4. Research results

4.1. Simulation results

4.1.1. Application of the proposed algorithm to evaluate the expanded measurement uncertainty

Simulations were conducted to evaluate the expanded uncertainty intervals of the effective value. The data generation procedure (Table 1) and the proposed algorithm (Table 2) were used for this purpose. The interval results were compared with those obtained using the classical MC method [6, 15]. The effects of the Gaussian noise, number of samples M, and frequency f on the interval results were examined. PTC Mathcad Prime software was used in this study. The data presented in Table 3 were inputted into the data generation procedure (Table 1) and proposed algorithm (Table 2).

The results showed the consistency of the expanded uncertainty intervals for the proposed algorithm and the classical MC method for all measurement cases considered in this study (Table 4 and Fig. 1). To distinguish the expanded uncertainty intervals in Table 4 for the different methods, the lower and upper endpoints (U_{low} and U_{high}) of the intervals are presented with three significant digits.

In this study, $p = 0.99$ was assumed to achieve a high reliability of the uncertainty evaluation results in simulations and experiments. This assumption was made to prevent underestimation of the uncertainty in the experiments. The proposed algorithm also allows the determination of the uncertainty for other values of p, such as $p = 0.95$.

Table 3. Input parameters for the procedure from Table 1 and the algorithm from Table 2.

Name	**Symbol**	**Set value**
Amplitude	V_m	9 V
Frequency	f	100−1100 Hz
Sampling frequency	f_s	12500 Hz
Number of samples	M	100−1000
Initial phase	φ	$\mathbf{R}[0, 2\pi]$
Zero error (offset)	ΔV_0^*	6.38 mV
Amplitude error	δV_m^*	0.0914%
Frequency error	δf^*	0.02%
Sampling frequency error	δf_s^*	0.01%
Number of repetitions	K	10^6
Coverage probability	p	0.99
Signal-to-noise ratio	SNR	40 dB

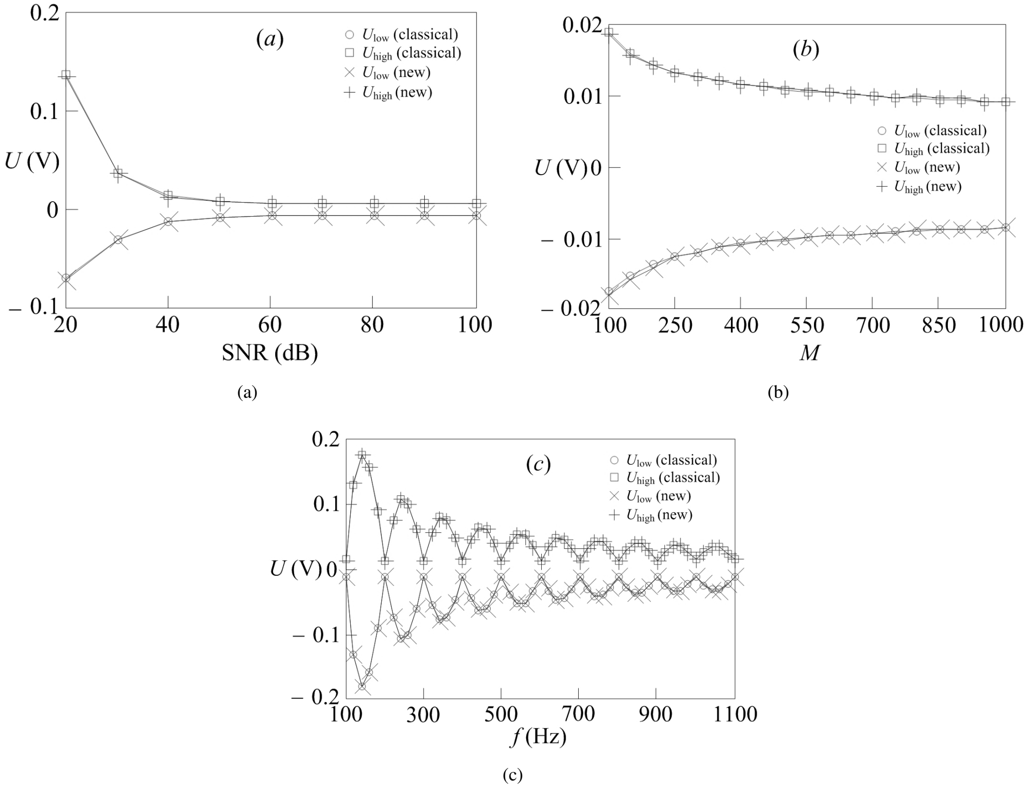

Fig. 1. Expanded uncertainty intervals as a function of SNR, M and f for (a) f = 500 Hz, M = 250, (b) f = 500 Hz, SNR = 40 dB, and (c) M = 250, SNR = 40 dB.

Table 4. Examples of expanded uncertainty intervals from Fig. 1.

			Classical MC method	New algorithm
Fig. 1a	SNR = 40 dB	U_{low} (mV)	−0.0129	−0.0127
		U_{high} (mV)	0.0135	0.0135
Fig. 1b	$M = 250$	U_{low} (mV)	−0.0129	−0.0132
		U_{high} (mV)	0.0133	0.0131
Fig. 1c	$f = 500$ Hz	U_{low} (mV)	−0.0126	−0.0126
		U_{high} (mV)	0.0133	0.0137

From the conducted research, it follows that:
– an increase in SNR and M results in a reduction of expanded uncertainty intervals (Figs. 1a and 1b),
– the smallest expanded uncertainty intervals are obtained under coherent sampling conditions, while failure to adhere to coherent sampling conditions leads to a significant increase in the intervals (Fig. 1c).

4.1.2. Application of the proposed algorithm for uncertainty budget determination

The proposed algorithm (Table 2) and classical MC method can be applied to construct an uncertainty budget for measuring the effective value of the sinusoidal voltage [6, 15]. To demonstrate this, we further conducted simulations concerning the measurement of the effective value using an exemplary measurement system. We assumed that in the measurement system an Agilent 33220A function generator was the voltage source, and voltage sampling was performed using a PCI 6024E data acquisition card. We also assumed that the voltage samples were transmitted to a computer, which calculated the effective value based on voltage samples and formula (7).

Table 5 presents the assumed parameter settings for the Agilent 33220A function generator, setting parameters for the PCI 6024E data acquisition card, and the limiting errors of these parameters obtained from the technical specifications of the instruments used. In addition, Table 5 provides information on the sources of noise present in the measured voltage. This enables the generation of noise with standard deviation:

$$\sigma_q = \sqrt{\left(\sigma_{\mathrm{G}}^*\right)^2 + \left(\sigma_{\mathrm{C}}^*\right)^2}, \tag{36}$$

where σ_{G}^* and σ_{C}^* are the standard deviations of the function generator noise and data acquisition card noise, respectively.

If the frequency of the signal is unknown, then it must be measured, and its accuracy must be determined to introduce these data into the proposed algorithm. If σ_{G} is unknown, then the type A uncertainty of the RMS voltage measurement, which is caused by random disturbances in the entire system, can be determined from a series of measurement results. In this case, the proposed algorithm allows the determination of type B uncertainty ($\sigma_q = 0$ is introduced into the algorithm).

Based on the data in Table 5, an uncertainty budget for measuring the effective value was created, as presented in Table 6. Similar to [6], the input quantities related to the limiting errors are presented in the simulated budget, namely, the standard uncertainties, probability distributions of these quantities, sensitivity coefficients, partial standard uncertainties (contributing to the combined uncertainty), and combined standard uncertainties.

Table 5. Parameters of the tested measurement system.

Name	Symbol	Set value
Voltage amplitude	V_m	9 V
Voltage frequency	f	500 Hz
Initial phase	φ	$\mathbf{R}[0, 2\pi]$
PCI card measurement range	V_{FS}	±10 V
Sampling frequency	f_s	12500 sps
Number of samples	M	250
Voltage frequency error	δf^*	0.02%
Standard deviation of noise in generator voltage	σ_G^*	2.02 mV (SNR = 70 dB)
PCI card A/D converter basic error	δV_m^*	0.0914%
PCI Card offset voltage	ΔV_0^*	6.38 mV
Standard deviation of noise in A/D converter voltage	σ_C^*	3.91 mV
PCI card time base error	δf_s^*	0.01%

The results confirmed the correctness of the proposed algorithm for evaluating the uncertainty because, for each source of uncertainty (input parameter), the results were similar to those obtained using the classical MC method. For both methods, the observed differences were at the level of repeatability of the simulations. Moreover, the obtained uncertainty budget confirmed the usefulness of the algorithm for evaluating the metrological properties of the measurement system. Based on the presented uncertainty budget, it can be deduced that in the analysed measurement case, the primary influence on the measurement uncertainty comes from the basic error of the data acquisition card (δV_m^*).

Table 6. Uncertainty budget of the effective value measurement for the tested measurement system.

Symbol	Quantity estimate	Standard uncertainty	Probability distribution	Sensitivity coefficient	New algorithm[1)]	Classical MC method[2)]
					u – contribution to the combined standard uncertainty (mV)	
δf	0 %	$0.02/\sqrt{3}$%	rectangular	2277 mV	0.263	0.263
σ_G	0 V	2.02 mV	normal	0.0634	0.128	0.128
δV_m	0 %	$0.0914/\sqrt{3}$%	rectangular	6367 mV	3.36	3.36
V_0	0 V	$6.38/\sqrt{3}$ mV	rectangular	0.0000863	0.000954	0.000954
σ_C	0 V	3.91 mV	normal	0.0632[1)]/0.0637[2)]	0.247	0.249
δf_s	0 %	$0.01/\sqrt{3}$%	rectangular	2269 mV	0.131	0.131
Δ_{RMS}	0.00 mV				3.39	3.39

4.2. Experimental results

Experiments were conducted to compare the measurement results of the effective value V_{RMS_PCI} obtained by the PCI 6024E data acquisition card and the uncertainties U_{low} and U_{high} obtained from simulations using the proposed algorithm with the measurement results of the effective value V_{RMS_HP} obtained by an HP 34401A multimeter with the expanded uncertainties U_{HP} determined by the uncertainty propagation method [14].

A measurement system, whose scheme is presented in Fig. 2, was constructed in this research. In this measurement system, sinusoidal voltage was generated using an Agilent 33220A function generator. This voltage was processed using two circuits. In one circuit, the voltage was sampled using a 12-bit A/D converter located on the PCI 6024E data acquisition card from which the sample values were sent to the computer memory. In the other circuit, the effective value was measured using an HP 34401A multimeter, and the measurement result was transmitted to the computer.

The computer memory included a measurement application developed in a LabWindows/CVI environment. The application allowed the configuration of both measurement devices (data acquisition card and multimeter), simultaneous start of measurements by both devices, reading of data from both devices, and computation of the effective value based on the voltage samples. The measurements were triggered by the software. In addition, the measurements were performed multiple times so that the scatter of the results could be considered in the uncertainty computations.

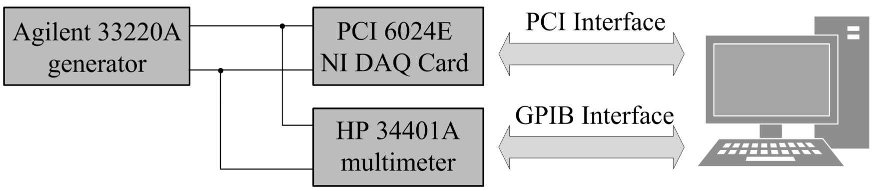

Fig. 2. Computer system for measuring the effective value using a PCI 6024E data acquisition card and an HP 34401A multimeter.

The results of the single measurements of effective values for the data acquisition card and multimeter ($V_{\mathrm{RMS\_PCI}}$ and $V_{\mathrm{RMS\_HP}}$) and the computed expanded measurement uncertainties are presented in Table 7. The measurements were conducted for different voltage frequencies set on the Agilent 33220A function generator, assuming that the voltage amplitude setting on the function generator and the processing parameters of the data acquisition card were consistent with those presented in Table 5. It can be observed that for frequencies of 50, 500, and 5000 Hz, theoretically coherent sampling of the voltage occurred, which was advantageous for the algorithm used to determine the RMS voltage. In other words, the smallest measurement uncertainties were obtained (see Section 4.1.1). However, the values of these set frequencies were biased by the function generator limit error δf^* with a value of 0.02%. For the other frequencies, the given frequency errors were larger because they were determined relative to the aforementioned frequencies treated as references. For example, for $f = 4990$ Hz, the relative error with respect to the nearest nominal value of 5000 Hz was −0.2%. Therefore, to evaluate the uncertainty interval (U_{low}, U_{high}) using the proposed algorithm, we assumed that the error δf^* was within ±0.2%. For the multimeter, the expanded measurement uncertainty was calculated using the following formula:

$$U_{\mathrm{HP}} = k_p \sqrt{\frac{\left(\Delta^*_{\mathrm{HP}}\right)^2}{3} + \left(\sigma_{V_{\mathrm{RMS\_HP}}}\right)^2}, \tag{37}$$

where Δ^*_{HP} was the measurement limiting error of the effective value, which was calculated based on the manufacturer's data of the multimeter ($\Delta^*_{\mathrm{HP}} = 0.06\%\ V_{\mathrm{RMS\_HP}} + 0.003$), $\sigma_{V\mathrm{RMS\_HP}}$ was the standard deviation determined based on 10 sequential results of $V_{\mathrm{RMS\_HP}}$, and $k_p = \sqrt{3}p$ was the coverage factor for the dominant rectangular distribution in the measurement and coverage probability of $p = 0.99$ [14].

The uncertainties presented in Table 7 were evaluated for a coverage probability of $p = 0.99$. This high value of p was deliberately chosen to avoid underestimating the uncertainty of the V_{RMS_PCI} measurement resulting from the fact that the actual error of f is at the limit of the assumed distribution of the error value δf used in the simulations to evaluate U_{low} and U_{high}.

To compare the measurement results and uncertainties for both instruments, the coverage intervals were determined, which are the ones that should contain the true effective value V_{true}. For measurements with the PCI 6024E data acquisition card, based on the simulated uncertainty intervals and measured voltages V_{RMS_PCI}, the coverage intervals $(V_{RMS\_PCI}+U_{low}, V_{RMS\_PCI}+U_{high})$ were determined analogous to those in [6, 18]. Meanwhile, for the HP 34401A multimeter, the coverage intervals were determined as $(V_{RMS\_HP} - U_{HP}, V_{RMS\_HP} + U_{HP})$. The results obtained for the considered measurement cases are summarised in Fig. 3.

Table 7. Measurement results and expanded uncertainties for $p = 0.99$.

Measurement case			PCI 6024E card			HP 34401A multimeter			
No	f (Hz)	δf^* (%)	V_{RMS_PCI} (V)	U_{low} (mV)	U_{high} (mV)	V_{RMS_HP} (V)	σV_{RMS_HP} (mV)	Δ^*_{HP} (mV)	U_{HP} (mV)
1	49.9	0.2	6.3584	−10.1	9.95	6.3503	0.094	6.9	6.8
2	49.95	0.1	6.3554	−7.7	7.7	6.3502	0.082	6.9	6.8
3	50	0.02	6.3581	−6.1	6.1	6.3501	0.061	6.9	6.8
4	499	0.2	6.3517	−10.1	10.1	6.3528	0.069	6.9	6.8
5	499.5	0.1	6.3571	−7.6	7.7	6.3529	0.086	6.9	6.8
6	500	0.02	6.3576	−6.1	6.1	6.3526	0.080	6.9	6.8
7	4990	0.2	6.3669	−22.9	23.0	6.3600	0.084	6.9	6.8
8	4995	0.1	6.3583	−15.3	15.6	6.3598	0.062	6.9	6.8
9	5000	0.02	6.3649	−7.5	7.6	6.3598	0.089	6.9	6.8

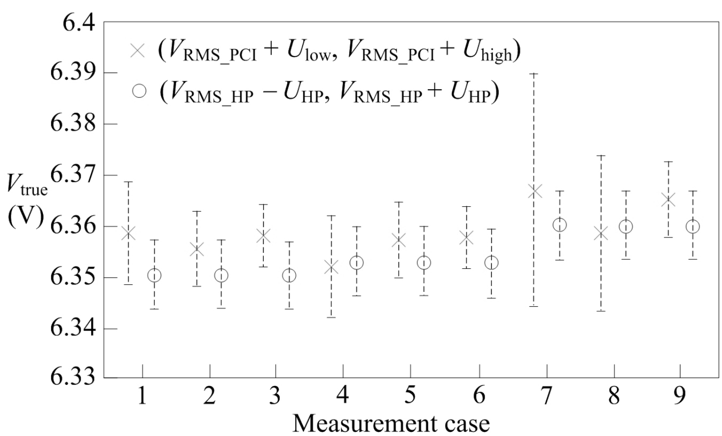

Fig. 3. Coverage intervals (intervals containing the true effective value V_{true}) for effective value measurements carried out using the PCI 6024E data acquisition card and HP 34401 multimeter for various measurement cases from Table 7.

DOI: 10.24425/mms.2023.154342

By analysing the obtained measurement results and computed uncertainties, their consistency could be observed. The coverage interval for the measurements performed using the PCI 6024E data acquisition card overlapped with the coverage interval obtained for the HP 34401 multimeter for each measurement case. This confirmed the correctness of the uncertainty calculations using the proposed algorithm. Furthermore, it can be noticed that under conditions closest to the coherent sampling ($\delta f^* = 0.02\%$), the measurement uncertainties of the voltage $V_{\mathrm{RMS\_PCI}}$ were comparable to the uncertainties for a commercial meter with relatively good metrological properties, such as the HP 34401A. A drawback of the digital algorithm for determining the RMS voltage is its sensitivity to non-coherent sampling, which is reflected in larger uncertainty intervals for larger errors of δf^*. A solution to this problem is to determine the frequency of the analysed alternating voltage based on its samples. Following this, for a voltage of theoretically any frequency, the number of samples M corresponding to the integer number of periods can be determined.

Subsequently, the effective value can be calculated based on these samples. In this case, the error δf^* can be determined from the relationship $\delta f_s^* + 1/M$. Hence, $\delta f^* = 0.02\%$ for $M = 10000$.

In summary, the experimental results confirmed the correct operation of the proposed algorithm in evaluating the measurement uncertainty of the effective value.

5. Time complexity study

A study to measure the time required to evaluate uncertainty intervals using both the new algorithm and the classical MC method was conducted. To do this, both algorithms were implemented in the Mathcad Prime computer program in the form of a dynamic worksheet [19]. The time measurements were performed using the function *time*() from Mathcad program. The created worksheet was run on a PC with a Windows 10 operating system equipped with an Intel Core i7−13700K processor and 32 GB of Kingston DDR5 6000 MHz RAM.

Figure 4 and Table 8 present the times required to evaluate uncertainty intervals obtained by averaging the results of 10 repetitions of the simulation. Each of the times consists of data generation time and algorithm execution time. The data generation time using the procedure from Table 1 is common for both algorithms. The research was conducted with voltage parameters and parameters of its digital processing as in Table 3.

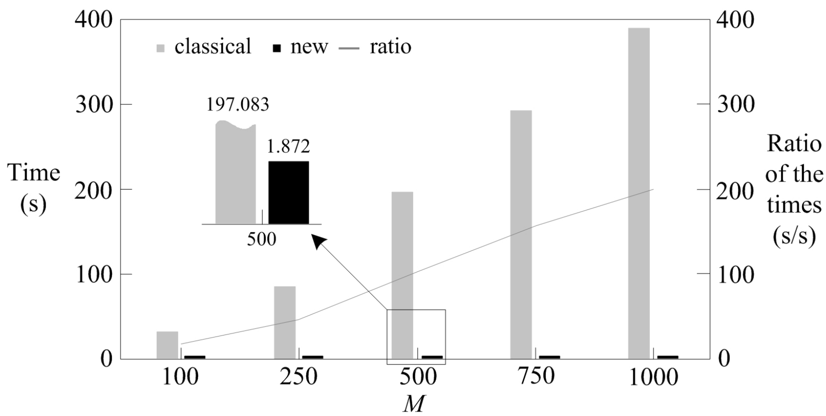

Fig. 4. Times of evaluating expanded uncertainty intervals expressed in seconds and ratio of the times.

Table 8. Times of evaluating expanded uncertainty intervals expressed in seconds.

Number of samples	Time for the classical MC method (s)	Time for the new algorithm (s)
$M = 100$	31.124	1.821
$M = 250$	86.398	1.894
$M = 500$	197.083	1.872
$M = 750$	294.343	1.864
$M = 1000$	390.624	1.943

The research results confirmed the high utility of the developed algorithm. Depending on M, the time required to evaluate a single uncertainty interval was from over 15 times (for $M = 100$) to over 200 times (for $M = 1000$) shorter than when using the classical MC method (ratio of the times in Fig. 4). The time to evaluate the uncertainty using the new algorithm depended only slightly on the number of samples M, whereas, in the case of the classical method, the computation time was strongly correlated with M.

6. Conclusions

This paper presents a new algorithm for fast uncertainty evaluation in digital measurements of effective voltage. The digital measurements are based on the acquisition of signal samples, which makes it difficult to use the uncertainty determination method based on the Guide [14]. Such measurements are easier to analyse using the classical MC method [15]. Even though this method is relatively easy to apply, it comes at the expense of long computational time. Our proposed algorithm is based on the MC method. Its advantage is its relatively simple implementation compared with uncertainty propagation method. At the same time, it is free from the disadvantages of the classical MC method and it can compute the measurement uncertainty within a significantly shorter time.

The algorithm presented in this paper makes it possible to evaluate the expanded uncertainty of the RMS voltage measurement as well as the combined standard uncertainty and partial standard uncertainties, which allows the creation of an uncertainty budget. The proposed algorithm provides a universal tool for analysing the metrological properties of any sample-based RMS voltage measurements. This paper presents the application of the proposed algorithm to an exemplary measurement system. However, the algorithm can be used in the metrological analysis of other measurement systems that are characterised by sources of uncertainty such as fundamental voltage measurement error, frequency error, sampling frequency error, zero error (offset), and noise. At the same time, the authors recommend using the developed algorithm in the coherent sampling mode. This is because the non-coherent sampling mode, resulting from the mismatch of the set sampling frequency of the A/D converter to the voltage frequency, is itself a source of uncertainty. The time required to evaluate the uncertainty is not dependent on the type of measurement system, but on the performance of the computer used. The ratio of the time required for the new algorithm to the time required for the classical MC method increased with an increase in the number of voltage samples. For example, for 1000 samples, the proposed algorithm was more than 200 times faster than the classical MC method.

The advantages of the proposed algorithm for evaluating the uncertainty in RMS voltage measurement indicate its potential as a software tool for analysing the properties of existing measurement systems. Moreover, this tool can be used in the design of new measurement systems, sampling voltmeters, wattmeters, and power network parameter meters which use digital RMS measurements based on voltage samples. Reducing the time required to evaluate uncertainty in the design process allows faster analysis of various design solutions. The significantly shorter time for evaluating the uncertainty also indicates the potential of implementing the proposed algorithm in the future, such as in sampling voltmeters, where the user can set the sampling parameters, and the voltmeter software will provide the measurement result along with its uncertainty.

References

[1] Croft, F. P. (2021). *American Electricians' Handbook*. 17Ed., McGraw Hill.

[2] Belega, D., & Găşpăresc, G. (2020). Accurate Measurement of the RMS of a Sine-wave by Means of Low-cost RMS-to-Dc converters. *Proceedings of the International Symposium on Electronics and Telecommunications*, Timisoara, Romania, 1–4. https://doi.org/10.1109/ISETC50328.2020.9301071

[3] Germer, H. (2001). High-precision AC measurements using the Monte Carlo method. *IEEE Transactions on Instrumentation and Measurement*, *50*(2), 457–460. https://doi.org/10.1109/19.918165

[4] Bulat, M., Mirković, S., Gazivoda, N., Pejić, D., Urekar, M., & Antić, B. (2024). An improved algorithm for the estimation of the root mean square value as an optimal solution for commercial measurement equipment. *Microprocessors and Microsystems*, *106*, 1–10. https://doi.org/10.1016/j.micpro.2024.105042

[5] Kostina, A. A., Tzvetkov, P. M., & Serov, A. N. (2020) Investigation of the method of RMS measurement based on moving averaging. *Proceedings of the 55th International Scientific Conference on Information, Communication and Energy Systems and Technologies*, Niš, Serbia, 235–238. https://doi.org/10.1109/ICEST49890.2020.9232779

[6] Krajewski, M. (2018). Constructing an uncertainty budget for voltage RMS measurement with a sampling voltmeter. *Metrologia*, *55*(11), 95–105. https://doi.org/10.1088/1681-7575/aaa178

[7] Novotny, M., & Sedlacek, M. (2008). RMS value measurement based on classical and modified digital signal processing algorithms. *Measurement*, *41*(3), 236–250. https://doi.org/10.1016/j.measurement.2006.11.011

[8] Novotny, M., & Slepicka, D. (2005). Uncertainty analysis of the phase and RMS value by non-coherent sampling in the frequency domain. *Proceedings of the IEEE Instrumentation and Measurement Technology Conference*, Ottawa, Canada, 2114–2117. https://doi.org/10.1109/IMTC.2005.1604547

[9] Hegeduš, H., Mostarac, P., & Malarić, R. (2011). Comparison of RMS value measurement algorithms of non-coherent sampled signals. *Measurement Science Review*, *11*(3), 79–84. http://www.measurement.sk/2011/Hegedus.pdf

[10] Muciek, A. K. (2007). A method for precise RMS measurements of periodic signals by reconstruction technique with correction. *IEEE Transactions on Instrumentation and Measurement*, *56*(2), 513–516. https://doi.org/10.1109/TIM.2007.891096

[11] Musiał, J., Horiashchenko, K., Horiashchenko, S., & Polasik, R. (2021). Modelling of diagnostics of the technical condition of cable lines and power supply systems. *Proceedings of the 20th International Conference Diagnostics of Machines and Vehicles*, *351*, 01008. https://doi.org/10.1051/matecconf/202135101008

[12] D'Apice, B., Landi, C., Pelvio, A., & Rignano. N. (2007). A multi-DSP based instrument for real-time energy and PQ measurements. *Metrology and Measurement Systems*, *14*(4) 495–506. http://www.metrology.pg.gda.pl/full/2007/M&MS_2007_495.pdf

[13] Baccigalupi, A., Darco, M., & Liccardo, A. (2017). Parameters and methods for ADCs testing compliant with the Guide to the expression of uncertainty in measurements. *IEEE Transactions on Instrumentation and Measurement*, *66*(3), 424–431. https://doi.org/10.1109/tim.2016.2644878

[14] Joint Committee for Guides in Metrology (2008). *Evaluation of measurement data – Guide to the expression of uncertainty in measurement* (JCGM 100:2008). https://www.bipm.org/documents/20126/2071204/JCGM_100_2008_E.pdf

[15] Joint Committee for Guides in Metrology (2008). *Evaluation of measurement data. Supplement 1 to the "Guide to the expression of uncertainty in measurement" – Propagation of distributions using a Monte Carlo method* (JCGM 101:2008). https://www.bipm.org/documents/20126/2071204/JCGM_101_2008_E.pdf

[16] Harris, P. M., & Cox, M. G. (2017). On a Monte Carlo method for measurement uncertainty evaluation and its implementation. *Metrologia*, *51*(4), 176–182. https://doi.org/10.1088/0026-1394/51/4/S176

[17] Bullen. P. S. (2003). *Handbook of Means and Their Inequalities*. Springer Science+Business Media, B.V. https://doi.org/10.1007/978-94-017-0399-4

[18] Otomański, P., & Fotowicz, P. (2011). Coverage interval as a measure of uncertainty of measurement. *Proceedings of the 8th International Conference on Measurement*, Smolenice, Slovakia, 3–6. https://www.measurement.sk/M2011/doc/proceedings/003_Otomanski-1.pdf

[19] Sienkowski, S., Krajewski, M., & Lal-Jadziak, J. Implementation of the developed algorithm in Mathcad Prime computer program. https://staff.uz.zgora.pl/ssienkow/apps/soft/uncertainty_rms.zip

[20] Cruywagen, G. C. (2023). Approximating the expectation and variance of the square root of the quadratic form in normal random variables. *Social Science Research Network, Elsevier*, 1–67. https://doi.org/10.2139/ssrn.4426554

[21] Hendeby, G., & Gustafsson, F. (2007). On nonlinear transformations of Gaussian distributions. *Technical Report from Automatic Control*, Linkoping University, Sweden. http://users.isy.liu.se/en/rt/fredrik/reports/07SSPut.pdf

Sergiusz Sienkowski is currently a professor at the Institute of Metrology, Electronics and Computer Science, University of Zielona Góra, Poland. He received his M.Sc. degrees from the Technical University of Zielona Góra, in 2001, and from the University of Zielona Góra in 2003. He received his Ph.D. degree in electrical engineering from the same university in 2011. His research activities focus on signal processing, processing of measured data, measuring circuits, evaluation of measurement uncertainty.

Mariusz Krajewski graduated with a M.Sc. in digital measuring circuits from the Technical University of Zielona Góra, Poland in 2001. He received his Ph.D. degree in electrical engineering from the Faculty of Electrical Engineering, Computer Science and Telecommunications of the University of Zielona Góra in 2009. Currently, he is working at that same faculty in the Institute of Metrology, Electronics and Computer Science as an assistant professor. His research interests focus on accurate electrical measurements, digital signal processing and evaluation of measurement uncertainty.

Jadwiga Lal-Jadziak received the M.Sc. and Ph.D. degrees in electrical engineering from the Wrocław University of Science and Technology, and Habilitate Doctorate (D.Sc.) degree from the Poznań University of Technology. She is the author or co-author of several dozen publications, including four monographs as well as three patents. Currently, she is employed as an associate professor in the Institute of Engineering and Technology, Nicolaus Copernicus University in Toruń. Her scientific interests include correlation techniques, measurements of random signals, estimation of signal characteristics, and randomised analog-to-digital processing.

Metrol. Meas. Syst., Vol. 32 (2025), No. 2, pp. 1–20
DOI: 10.24425/mms.2023.154342

APPENDIX

A. Variance and bias of the effective value estimator

The variance of the RMS_e estimator from formula (7) of the RMS parameter from formula (8) can be calculated as follows (20):

$$\operatorname{Var}\left[RMS_e\right] \approx \sigma_q^2 \sum_{n=0}^{M-1} \left(\frac{\partial}{\partial v_0\left[n\right]} \hat{m}\left(\mathbf{w_0}, 2\right) \right)^2, \tag{A.1}$$

where:

$$\mathbf{w_0} = \left[v_0\left[0\right] + V_0 + \mu_q \ \mathrm{L} \ v_0\left[M-1\right] + V_0 + \mu_q \right]^T \tag{A.2}$$

and:

$$\begin{aligned} \hat{m}\left(\mathbf{w_0}, 2\right) &= \sqrt{\frac{1}{M} \sum_{n=0}^{M-1} \left(v_0\left[n\right] + V_0 + \mu_q\right)^2} \\ &= \sqrt{\left(V_0 + \mu_q\right)^2 + \left(\hat{m}\left(\mathbf{v_0}, 2\right)\right)^2 + 2\left(V_0 + \mu_q\right) \hat{m}\left(\mathbf{v_0}, 1\right)}. \end{aligned} \tag{A.3}$$

At the same time:

$$\begin{aligned} &\frac{\partial}{\partial v_0\left[0\right]} \hat{m}\left(\mathbf{w_0}, 2\right) = \frac{v_0\left[0\right] + V_0 + \mu_q}{M \hat{m}\left(\mathbf{w_0}, 2\right)}, \\ &\mathrm{K}, \frac{\partial}{\partial v_0\left[M-1\right]} \hat{m}\left(\mathbf{w_0}, 2\right) = \frac{v_0\left[M-1\right] + V_0 + \mu_q}{M \, \hat{m}\left(\mathbf{w_0}, 2\right)}. \end{aligned} \tag{A.4}$$

Then:

$$\begin{aligned} \operatorname{Var}\left[RMS_e\right] &\approx \sigma_q^2 \left(\frac{\left(v_0\left[0\right] + V_0 + \mu_q\right)^2}{M^2 \left(\hat{m}\left(\mathbf{w_0}, 2\right)\right)^2} + \mathrm{K} + \frac{\left(v_0\left[M-1\right] + V_0 + \mu_q\right)^2}{M^2 \left(\hat{m}\left(\mathbf{w_0}, 2\right)\right)^2} \right) \\ &= \frac{\sigma_q^2}{M \left(\hat{m}\left(\mathbf{w_0}, 2\right)\right)^2} \frac{1}{M} \sum_{n=0}^{M-1} \left(v_0\left[n\right] + V_0 + \mu_q\right)^2 = \frac{\sigma_q^2}{M}. \end{aligned} \tag{A.5}$$

The bias of the RMS_e estimator is equal to:

$$\mathrm{b}\left[RMS_e\right] \approx \hat{m}\left(\mathbf{w_0}, 2\right) + \frac{\sigma_q^2}{2} \sum_{n=0}^{M-1} \left(\frac{\partial^2}{\partial^2 v_0\left[n\right]} \hat{m}\left(\mathbf{w_0}, 2\right) \right) - RMS. \tag{A.6}$$

Since:

$$\begin{aligned} &\frac{\partial^2}{\partial^2 v_0\left[0\right]} \hat{m}\left(\mathbf{w_0}, 2\right) = \frac{1}{M \, \hat{m}\left(\mathbf{w_0}, 2\right)} - \frac{\left(v_0\left[0\right] + V_0 + \mu_q\right)^2}{M^2 \left(\hat{m}\left(\mathbf{w_0}, 2\right)\right)^3}, \\ &\qquad \vdots \\ &\frac{\partial^2}{\partial^2 v_0\left[M-1\right]} \hat{m}\left(\mathbf{w_0}, 2\right) = \frac{1}{M \hat{m}\left(\mathbf{w_0}, 2\right)} - \frac{\left(v_0\left[M-1\right] + V_0 + \mu_q\right)^2}{M^2 \left(\hat{m}\left(\mathbf{w_0}, 2\right)\right)^3}, \end{aligned} \tag{A.7}$$

then:

$$\mathrm{b}\left[\mathrm{RMS_e}\right] \approx \hat{\mathrm{m}}\left(\mathbf{w_0}, 2\right) - \mathrm{RMS} + \frac{\sigma_q^2}{2}\left(\frac{1}{M\hat{\mathrm{m}}\left(\mathbf{w_0}, 2\right)} - \frac{\left(v_0\left[0\right] + V_0 + \mu_q\right)^2}{M^2\left(\hat{\mathrm{m}}\left(\mathbf{w_0}, 2\right)\right)^3}\right)$$
$$+ \ldots + \frac{\sigma_q^2}{2}\left(\frac{1}{M\hat{\mathrm{m}}\left(\mathbf{w_0}, 2\right)} - \frac{\left(v_0\left[M-1\right] + V_0 + \mu_q\right)^2}{M^2\left(\hat{\mathrm{m}}\left(\mathbf{w_0}, 2\right)\right)^3}\right). \tag{A.8}$$

Thus:

$$\mathrm{b}\left[\mathrm{RMS_e}\right] \approx \hat{\mathrm{m}}\left(\mathbf{w_0}, 2\right) - \mathrm{RMS} + \frac{\sigma_q^2}{2}\frac{1}{\hat{\mathrm{m}}\left(\mathbf{w_0}, 2\right)}$$
$$- \frac{\sigma_q^2}{2M}\frac{1}{M\left(\hat{\mathrm{m}}\left(\mathbf{w_0}, 2\right)\right)^3}\sum_{n=0}^{M-1}\left(v_0\left[n\right] + V_0 + \mu_q\right)^2$$
$$= \hat{\mathrm{m}}\left(\mathbf{w_0}, 2\right) + \frac{\sigma_q^2}{2\hat{\mathrm{m}}\left(\mathbf{w_0}, 2\right)}\left(1 - \frac{1}{M}\right) - \mathrm{RMS}. \tag{A.9}$$

Substituting (A.3) into (A.9), we obtain:

$$\mathrm{b}\left[\mathrm{RMS_e}\right] \approx \sqrt{\left(V_0 + \mu_q\right)^2 + \left(\hat{\mathrm{m}}\left(\mathbf{v_0}, 2\right)\right)^2 + 2\left(V_0 + \mu_q\right)\hat{\mathrm{m}}\left(\mathbf{v_0}, 1\right)} - \mathrm{RMS}$$
$$+ \frac{\sigma_q^2}{2\sqrt{\left(V_0 + \mu_q\right)^2 + \left(\hat{\mathrm{m}}\left(\mathbf{v_0}, 2\right)\right)^2 + 2\left(V_0 + \mu_q\right)\hat{\mathrm{m}}\left(\mathbf{v_0}, 1\right)}}\left(1 - \frac{1}{M}\right). \tag{A.10}$$

From (13) and (14) it follows that:

$$\rho_m = \hat{\mathrm{m}}\left(\mathbf{v_0}, 1\right), \rho_P = \left(\hat{\mathrm{m}}\left(\mathbf{v_0}, 2\right)\right)^2. \tag{A.11}$$

Then:

$$\mathrm{b}\left[\mathrm{RMS_e}\right] \approx \sqrt{\left(V_0 + \mu_q\right)^2 + \rho_P + 2\left(V_0 + \mu_q\right)\rho_m} - \mathrm{RMS}$$
$$+ \frac{\sigma_\mathrm{q}^2}{2\sqrt{\left(V_0 + \mu_q\right)^2 + \rho_P + 2\left(V_0 + \mu_q\right)\rho_m}}\left(1 - \frac{1}{M}\right). \tag{A.12}$$

The formula (A.12) can be transformed into the following form:

$$\mathrm{b}\left[\mathrm{RMS_e}\right] \approx \sqrt{\mu_q^2 + \mathrm{P}_v + 2\mu_q \mathrm{m}_v} - \mathrm{RMS} + \frac{\sigma_q^2}{2\sqrt{\mu_q^2 + \mathrm{P}_v + 2\mu_q \mathrm{m}_v}}\left(1 - \frac{1}{M}\right), \tag{A.13}$$

where P_v is given by the formula (14), while:

$$\mathrm{m}_v = V_0 + \rho_m. \tag{A.14}$$

B. Variance of the mean power estimator

In order to calculate the variance of the estimator P from formula (12) of the power P_{v0} from formula (9), we use the formula (21):

$$\begin{aligned}\mathrm{Var}\,[\mathrm{P}] \approx \sigma_q^2 \sum_{n=0}^{M-1} \left(\frac{\partial}{\partial v_0\,[n]} \left(\hat{\mathrm{m}}\left(\mathbf{w_0}, 2\right)\right)^2 \right)^2 + \frac{\sigma_q^4}{2} \sum_{n=0}^{M-1} \left(\frac{\partial^2}{\partial^2 v_0\,[n]} \left(\hat{\mathrm{m}}\left(\mathbf{w_0}, 2\right)\right)^2 \right)^2 \\ + \sigma_q^4 \sum_{n=0}^{M-1} \frac{\partial}{\partial v_0\,[n]} \left(\hat{\mathrm{m}}\left(\mathbf{w_0}, 2\right)\right)^2 \frac{\partial^3}{\partial^3 v_0\,[n]} \left(\hat{\mathrm{m}}\left(\mathbf{w_0}, 2\right)\right)^2,\end{aligned} \tag{B.1}$$

where $\hat{\mathrm{m}}\left(\mathbf{w_0}, 2\right)$ is given by the formula (A.3). Hence:

$$\begin{aligned}\frac{\partial}{\partial v_0\,[0]} \left(\hat{\mathrm{m}}\left(\mathbf{w_0}, 2\right)\right)^2 &= \frac{2}{M} \left(v_0\,[0] + V_0 + \mu_q\right), \\ &\vdots \\ \frac{\partial}{\partial v_0\,[M-1]} \left(\hat{\mathrm{m}}\left(\mathbf{w_0}, 2\right)\right)^2 &= \frac{2}{M} \left(v_0\,[M-1] + V_0 + \mu_q\right),\end{aligned} \tag{B.2}$$

$$\frac{\partial^2}{\partial^2 v_0\,[0]} \left(\hat{\mathrm{m}}\left(\mathbf{w_0}, 2\right)\right)^2 = \frac{2}{M}, \ldots, \frac{\partial^2}{\partial^2 v_0\,[M-1]} \left(\hat{\mathrm{m}}\left(\mathbf{w_0}, 2\right)\right)^2 = \frac{2}{M}, \tag{B.3}$$

$$\frac{\partial^3}{\partial^3 v_0\,[0]} \left(\hat{\mathrm{m}}\left(\mathbf{w_0}, 2\right)\right)^2 = 0, \ldots, \frac{\partial^3}{\partial^3 v_0\,[M-1]} \left(\hat{\mathrm{m}}\left(\mathbf{w_0}, 2\right)\right)^2 = 0, \tag{B.4}$$

then:

$$\begin{aligned}\mathrm{Var}\,[\mathrm{P}] \approx \sigma_q^2 \left(\frac{4}{M^2} \left(v_0\,[0] + V_0 + \mu_q\right)^2 + \ldots + \frac{4}{M^2} \left(v_0\,[M-1] + V_0 + \mu_q\right)^2 \right) \\ + \frac{\sigma_q^4}{2} \left(\frac{4}{M^2} + \ldots + \frac{4}{M^2} \right) = \sigma_q^2 \left(\frac{4}{M} \left(\frac{1}{M} \sum_{n=0}^{M-1} \left(v_0\,[n] + V_0 + \mu_q\right)^2 \right) \right) + \frac{2\sigma_q^4}{M}.\end{aligned} \tag{B.5}$$

Therefore:

$$\begin{aligned}\mathrm{Var}\,[\mathrm{P}] \approx \sigma_q^2 \left(\frac{4}{M} \left(\left(V_0 + \mu_q\right)^2 + \frac{1}{M} \sum_{n=0}^{M-1} \left(v_0\,[n]\right)^2 + 2\left(V_0 + \mu_q\right) \frac{1}{M} \sum_{n=0}^{M-1} v_0\,[n] \right) \right) \\ + \frac{2\sigma_q^4}{M} = \frac{4\sigma_q^2}{M} \left(\left(V_0 + \mu_q\right)^2 + \left(\hat{\mathrm{m}}\left(\mathbf{v_0}, 2\right)\right)^2 + 2\left(V_0 + \mu_q\right) \hat{\mathrm{m}}\left(\mathbf{v_0}, 1\right) \right) + \frac{2\sigma_q^4}{M}.\end{aligned} \tag{B.6}$$

At the same time, it follows from (A.11) that:

$$\mathrm{Var}\,[\mathrm{P}] \approx \frac{4\sigma_q^2}{M} \left(\left(V_0 + \mu_q\right)^2 + \rho_P + 2\left(V_0 + \mu_q\right) \rho_m \right) + \frac{2\sigma_q^4}{M}. \tag{B.7}$$

Then:

$$\sigma_P = \sqrt{\mathrm{Var}\,[\mathrm{P}]} = \frac{2}{\sqrt{M}} \sigma_q \sqrt{\left(V_0 + \mu_q\right)^2 + \rho_P + 2\left(V_0 + \mu_q\right) \rho_m + \frac{1}{2}\sigma_q^2}. \tag{B.8}$$

The above formula can be transformed into the following form:

$$\sigma_P = \frac{2}{\sqrt{M}}\sigma_q\sqrt{\mu_q^2 + \mathrm{P}_v + 2\mu_q \mathrm{m}_v + \frac{1}{2}\sigma_q^2}, \tag{B.9}$$

where P_v and m_v are given by the formulas (14) and (A.14).